Available online at www.sciencedirect.com
SCIENCE DIRECT
Tectonophysics 420 (2006) 123–140
TECTONOPHYSICS
www.elsevier.com/locate/tecto

Deep seismic investigation across the Barents–Kara region and Novozemelskiy Fold Belt (Arctic Shelf)

N.M. Ivanova *, T.S. Sakoulina, Yu.V. Roslov

State Company "SEVMORGEO", Rosenshtein Str.36, 198095, St. Petersburg, Russia

Received 17 January 2005; received in revised form 7 October 2005; accepted 4 January 2006
Available online 11 April 2006

Abstract

Since 1995 SEVMORGEO has collected wide-angle reflection/refraction profiling (WARRP), multichannel seismic data (MCS) and seismoacoustic profiling, along regional lines 1-AR, 2-AR and 3-AR. These lines cross the whole Barents–Kara Region and Novozemelskiy Fold Belt. As a result, new geological data about the deep structure of the Earth's crust have become available. Four main tectono-stratigraphic units are distinguished in the section of the Earth's crust: (1) a sedimentary cover; (2) the Upper Proterozoic (mainly Riphean for the Barents Plate) and Riphean–Paleozoic (the South-Kara Syneclise) deformed and folded complexes; (3) the upper crystalline crust (granite-gneissic metamorphic Archean–Proterozoic complex); (4) the lower crust (basalt complex). The Barents–Kara Region is characterized by moderately thinned continental and subcontinental crust with an average thickness of 37–39 km. On islands and areas of uplifts with ancient massifs, the thickness of the crust (38–42 km) approaches the typical crust for a continental platform. In the Novozemelskiy Fold Belt the thickness of the crust reaches 40–42 km. Rift-related grabens are characterized by significant crustal thinning with thicknesses of 33–36 km. Several grabens are revealed: the Riphean Graben on the Kola-Kanin Monocline, the Lower Paleozoic West-Kola Graben, the Devonian Demidovskiy Aulacogen, the Upper Paleozoic Malyginskiy Graben in the Barents Region and Upper Paleozoic–Triassic Noyabr'skiy and the Chekinskiy grabens in the Kara Region. Data concerning the deep structure lead us to conclude that mainly destructive processes contributed to the dynamics of the forming of the Barents–Kara Region.

Keywords: Seismic investigations; Wide-angle refraction/reflection; Barents–Kara Region; Crust; Sedimentary cover; Complex; Rift; Graben

1. Introduction

Geophysical data, including wide-angle reflection/refraction profiling (WARRP) (SEVMORGEO, St. Petersburg, RAS Institute of the Physics of the Earth, Moscow), multi-channel seismic — MCS (Marine Arctic Geological Expedition — MAGE), Sevmorneftegeofizika — SMNG, Murmansk), Wide Aperture Deep Seismic Profiling — WADSP (MAGE, VNIIOkeangeologia, St. Petersburg) and gravity/magnetic measurements, have been interpreted to study a deep geological structure of the Barents–Kara Region.

Since 1995 SEVMORGEO has carried out seismic investigations, including WARRP, MCS and high-frequency profiling, along regional lines 1-AR, 2-AR (Fig. 1). Gravity and magnetic measurements were also completed along these lines. Line 1-AR (1440 km total length with 1330 km at sea and 110 km on land) connects the superdeep hole-3 on the Kola Peninsula (town of Zapolarny) with the hole 1-Hayes on Franz Joseph Land. Line 2-AR (935 km long) traverses the

* Corresponding author.
E-mail address: ivanova@sevmorgeo.com (N.M. Ivanova).

0040-1951/$ - see front matter © 2006 Elsevier B.V. All rights reserved.
doi:10.1016/j.tecto.2006.01.011

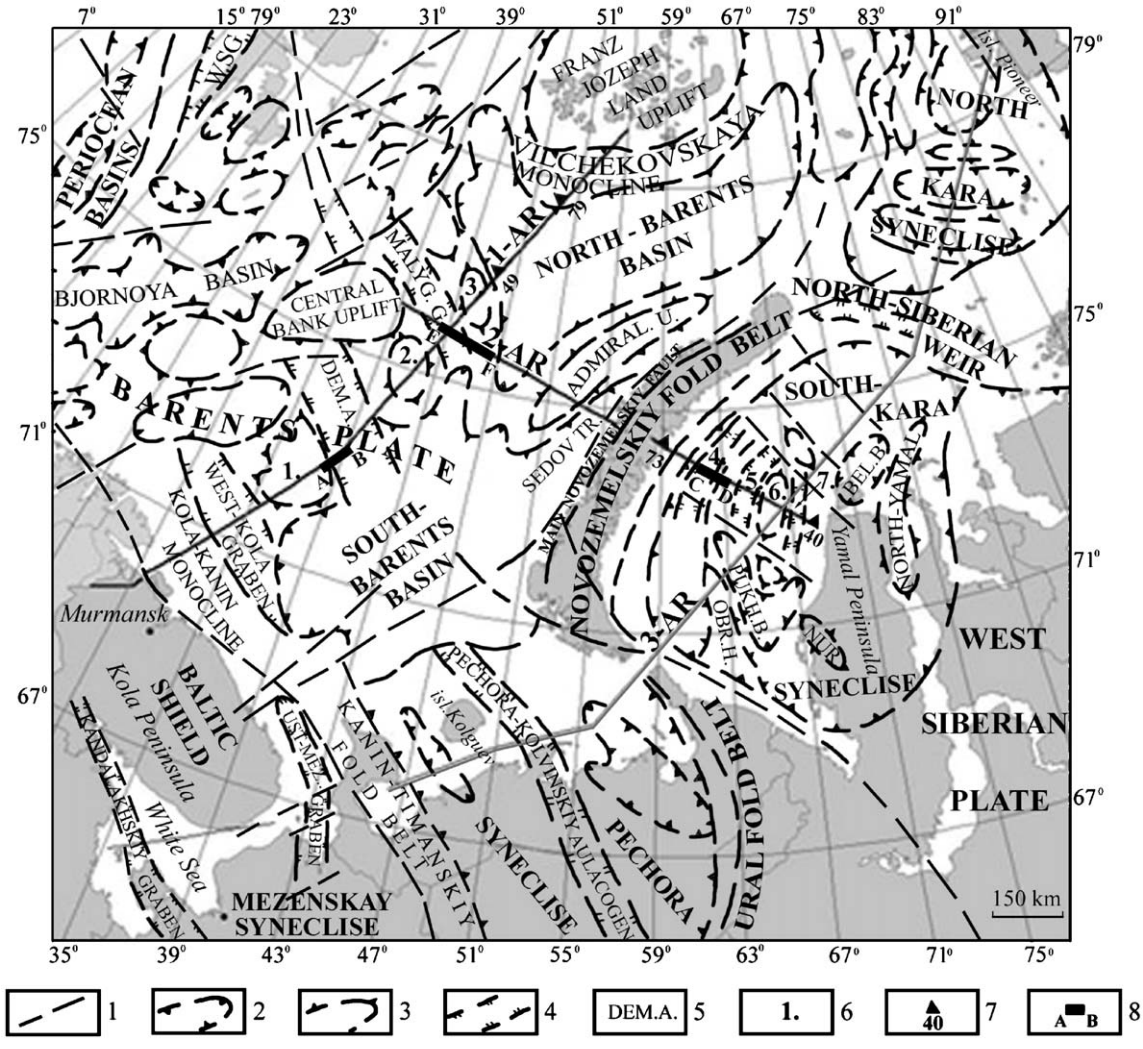

Fig. 1. Regional lines location scheme on the tectonic background. 1, Main faults; 2, boundaries of basins; 3, boundaries of uplifts or highs; 4, grabens or Aulacogen; 5, shortened name of structural elements on the scheme: DEM. A. — Demidovskiy Aulacogen, MALYG. G. — Malyginskiy graben, UST-MEZ. — Ust-Mezenskiy Graben, WSG — West-Spitsbergen Graben, NUR. — Nurminskiy High, OBR. H. — Obruchevskiy High, PUKH. B. — Pukhuchanskiy Basin, Bel. B. — Beloostrobskiy Basin; 6, main uplifts and graben structures along regional lines 1-AR, 2-AR: 1. — Fedynskiy Uplift, 2. — Fersmanovskiy Uplift, 3. — Vernadskiy Uplift, 4. — Pakhtusovskiy Trough, 5. — Noyabr'skiy Graben, 6. — Rusanovskiy High, 7. — Chekinskiy Graben; 7, location of wavefield examples (WARRP) with number of sounding; 8, location of fragments of MCS lines.

Kara Shelf–Island Novaya Zemlya–central part of the Barents Shelf. In 2003 SEVMORGEO started seismic investigations and gravity/magnetic measurements along regional line 3-AR, connecting the White Sea with the Island Pioneer (the north part of the Kara Sea). In this article emphasis will be on new geological results along lines 1-AR and 2-AR. The data of previous investigations on a belt of width 200 km were used to construct a deep model of Earth's crust along regional lines 1-AR and 2-AR (Verba et al., 1999; Sakoulina et al., 2003). These geotraverses, crossing the whole continental margin of the northern Europe, serve to link two transcontinental profiles systems — in the south implemented by the EUROPROBE project, and in the Arctic Ocean — by the TRANSARCTICA project (Sakoulina et al., 2000).

The Arctic Shelf of Russia has not been studied enough to elucidate the crustal dynamics and evolution in continent–ocean transition zones, requiring further deep investigations in this region. Previous geological

and geophysical research in the Barents–Kara Region indicated its oil and gas potential and led to the discovery of several large fields (Shtokmanovskoe, Ledovoe, Ludlovskoe, Prirazlomnoe and others on the Barents Shelf; Rusanovskoe, Leningradskoe on the Kara Shelf) (Fedorovckiy et al., 1993). New information about deep Paleozoic complexes of sedimentary cover is important for a common valuation of hydrocarbon potential of the region. The geotraverses cover the junction zone of the Barents Plate, Novozemelskiy Fold Belt and an offshore part the West-Siberian Plate (the South-Kara Syneclise). These structures differ by age and composition of sedimentary cover, depths of crystalline basement and crustal thickness. The WARRP survey of SEVMORGEO also provides new data concerning the deep (collisional) structure of the Novozemelskiy Fold Belt.

The Barents–Kara Region has a compound structure, with a thick sedimentary cover, a heterogeneous basement and is complicated by rift structures. The detailed tectonic structure of the Barents–Kara Region is mainly associated with repeated rifting. Therefore, the major objective was to study the topography and physical parameters of the granite-gneissic metamorphic complex and to determinate the age and composition of synrift complexes. The purpose of this article is to illustrate the special features of the deep structure of the Barents–Kara Region from recent deep seismic investigations.

2. Geological setting

The territory considered covers the area of the Barents Plate, Novozemelskiy Fold Belt and an offshore part the West-Siberian Plate (the South-Kara Syneclise). The sedimentary cover of the Barents Plate is composed mainly of Paleozoic terrigenous–carbonate sediments and Mesozoic terrigenous deposits. Almost synchronous to them in age, sedimentary and subordinate magmatic and metamorphic rocks, deformed in folds and complicated by faults, are exposed within the Novozemelskiy Fold Belt. Probably they form folded basement in the adjoining area of the West-Siberian Plate (Novaya Zemlya Island). The West-Siberian Plate is characterized by gently dipping terrigenous, mainly Triassic–Neogene deposits (Kunin and Joganson, 1982). The sedimentary basins of the Barents and Kara Shelf are the largest shelf structures of the Arctic region and are a part of the enormous area of the Mesozoic sedimentation, which spreads all over the western Arctic continental Margin (Gramberg et al., 1988). Formed in the Early Cimmerian Epoch, the Novozemelskiy Fold Belt separates sedimentary basins of the Barents Shelf (west) and Kara Shelf (east).

Geophysical investigations have shown the Barents Plate to consist of mobile zones with relatively thin crust and an area of carbonate platforms with thick crust. The mobile zones are rift related, as in the South-Barents Basin and North-Barents Basin, where mainly the Upper Paleozoic–Mesozoic terrigenous deposits (up to 14–18 km) form the sedimentary cover (Ivanova, 1997). Carbonate platforms are characterized by a reduced thickness of Upper Paleozoic (mainly Permian)–Mesozoic terrigenous sediments (up to 2–8 km) and relatively stable thickness of Paleozoic terrigenous and carbonate rocks (4–6 km). The main structural elements, which were formed through the geological history, include such large structures in the Barents Plate, as the South-Barents Basin, North-Barents Basin, Kola-Kanin Monocline, West Kola Graben, Central Barents Zone of uplifts (the Fedynskiy, Fersmanovskiy, Central Bank, Vernadskiy uplifts), complicated by the Demidovskiy and Malyginskiy graben structures. Other elements include the Vilchekovskaya Monocline, which represents a transition zone between the North-Barents Basin and Frantz Joseph Land Uplift; Admiralteyskiy Uplift, and the Trough Sedov (Fig. 1). The margin-continental Barents Plate has mainly continental type of Earth crust, although in some limited areas crustal thickness decreases to 25–30 km is fixed (Gramberg et al., 1988). The deep structure of large parts of the Barents Plate remained almost unknown until recently.

Structural complexes of various ages form a basement of the Barents Plate. They are: the Karelian complex of Early Proterozoic age composing the northeast slope of the Baltic Shield and dipping beneath the Barents Sea; the variably reactivated Baikalian complex of Late Proterozoic age (mainly in the Pechora Syneclise); problematic continuations of zones of Caledonian fold-block dislocations; Hercynian and Cimmerian complexes of Ural and Novozemelskiy Fold Belt (Shipilov and Senin, 1988).

The Novozemelskiy Fold Belt is a part the Paikhoy–Novozemelskiy folding system located on periphery of the Ural Fold Belt. The Novozemelskiy Fold Belt was formed in Early Mesozoic, during the Jurassic–Early Triassic collision. The Main Novozemelskiy Fault is a major structural element of the Novozemelskiy Fold Belt. The West-Novozemelskaya Zone of thrust-overfault dislocations forms the western part of the Novozemelskiy Fold Belt (Korago et al., 1992). The northeastern continuation of the Novozemelskiy Fold Belt is represented by folding structures of the North-Siberian Weir (Fig. 1).

The West-Siberian Plate represents the largest Mesozoic–Cenozoic basin, overlaying a basement of diverse structures of ancient platforms and fold belts (Kunin and Joganson, 1982). The South-Kara Syneclise represents the northern offshore continuation of the West-Siberian Plate. The structure of the central South-Kara Syneclise is formed by a conjugate system of graben-like troughs and uplifts, extending mainly in northeasterly and northwesterly directions (Ivanova, 1998). By analyzing refraction seismic data in the most subsided part of the Syneclise, pre-Mesozoic complexes are identified between the Proterozoic basement and the latter sedimentary cover. The inner structures of the South-Kara Syneclise include large highs (the Obruchevskiy, Rusanovskiy, North-Yamal, Nurminskiy and other), where the maximum thickness of sedimentary cover is 5–7 km, and deep graben structures (the Pukhuchanskiy, Beloostrovskiy basins, Noyabr'skiy, Chekinskiy grabens and other) with the thickness sedimentary cover up to 7–14 km (Ivanova and Kavoun, 1996; Ivanova, 1998).

3. Data acquisition

Observations on the lines 1-AR and 2-AR included various geophysical methods, consisting of various seismic investigations, in particular, reflection multichannel seismic (MCS) and wide-angle reflection/refraction profiling (WARRP), and onboard gravity/magnetic observations. In addition, on 1-AR aeromagnetic measurements within a 100 km strip were carried out and on 2-AR, seismoacoustic (high-frequency) profiles were acquired.

WARRP observations have been recorded with a reversed acquisition geometry using a spread of ocean bottom stations (OBS) and shooting by powerful air-gun. Seismic signals were recorded by digital four-component OBSs developed by the Sevmorgeo (St. Petersburg) and the Tekhmorgeo (Murmansk). Each OBS provides four-component registration with 3 geophones and hydrophone. One geophone is oriented in vertical direction and the others are located in the horizontal plane. On 1-AR the analog four-component recording instruments developed by the Oceanology Institute of Russian Academy of Sciences (Moscow) were also applied. Records of refracted/reflected waves were mostly obtained at offsets of 150–180 km (280–320 km at several points). On the land segment (110 km) of the line, stations Zemlya-M were installed very irregularly at 9 points, with their spacing ranging from 2 to 67 km.

Reflection MCS observations have been executed by Sevmorneftegeofizika (Murmansk). The MCS technique has enabled studying all basic horizons in the sedimentary cover; reflecting boundaries are traced in the time interval from 0 up to 8 s.

Table 1
Registration parameters

	1-AR		2-AR	
Line length	1440		935	
WARRP	*Offshore*	*Onshore*	*Barents Sea*	*Kara Sea*
Number of stations	90	9	56	45
Station space (km)	5–10–20–40	2–67	2.5–20	2.5–20
Air-gun volume (cubic inches)	4900; 7300	4900; 7300	7300	7300
Shot space (m)	250	250	250	
Record length (s)	60		60	
Reflection MCS				
Segment line length	1451		380	294
Number of channels	360		480	
Channel interval (m)	12.5		12.5	
Record length (s)	14		14	
Maximum offset (m)	4647.5		6087.75	
Fold	45		80	
Air-gun volume (cubic inches)	2280		4736	
Shot space (m)	50		37.5	

WARRP and MCS registration parameters are shown in the Table 1. We note, that

(1) on 1-AR, stations deployed on onshore segment registered offshore air-gun source;
(2) on 2-AR, OBSs in the Barents Sea near to Novozemelskiy Fold Belt recorded the seismic waves from air-gun shots in the western part of Kara Sea and the opposite for the reversed shots.

4. Data processing and interpretation

4.1. WARRP data

4.1.1. A general characteristic of the wave field on lines 1-AR and 2-AR

The waves associated with boundaries in the sedimentary cover, basement, horizons inside consolidated crust and the Moho discontinuity have been tracked on seismic records.

Note the following basic features of the records for offshore segments of lines 1-AR (Fig. 2) and 2-AR (Fig. 3).

1. The waves associated with the Moho, have mostly steady character. Strong near-critical reflections (Pm) from the base of an Earth's crust — Moho are

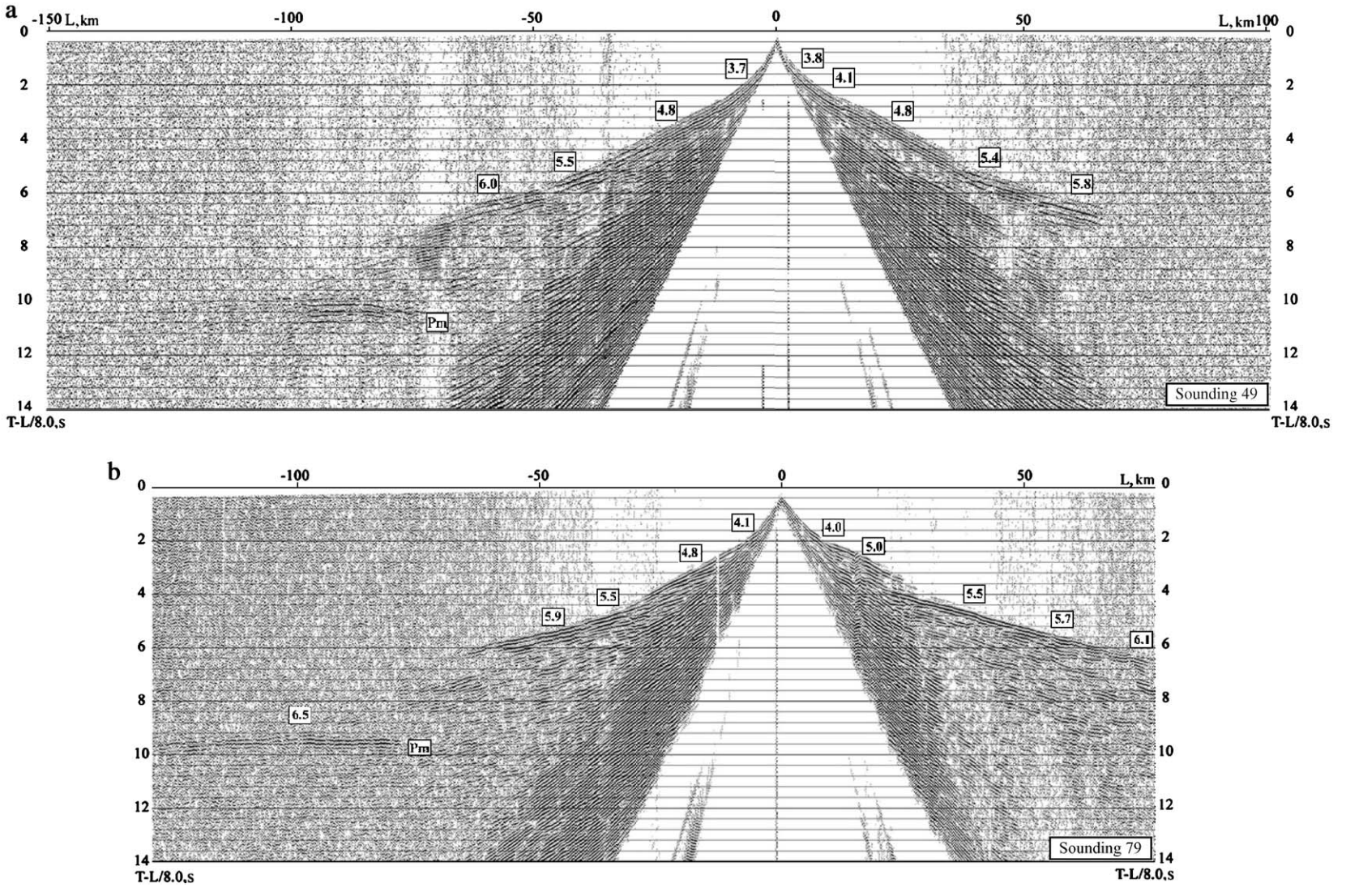

Fig. 2. Examples of wavefields: (a) Line 1-AR, Barents Sea sounding 49, a line distance of 950 km; (b) Line 1-AR, Barents Sea, sounding 79, a line distance of 1250 km. Reduction velocity 8 km·s^{-1}. Values in squares — apparent velocities in km s^{-1}.

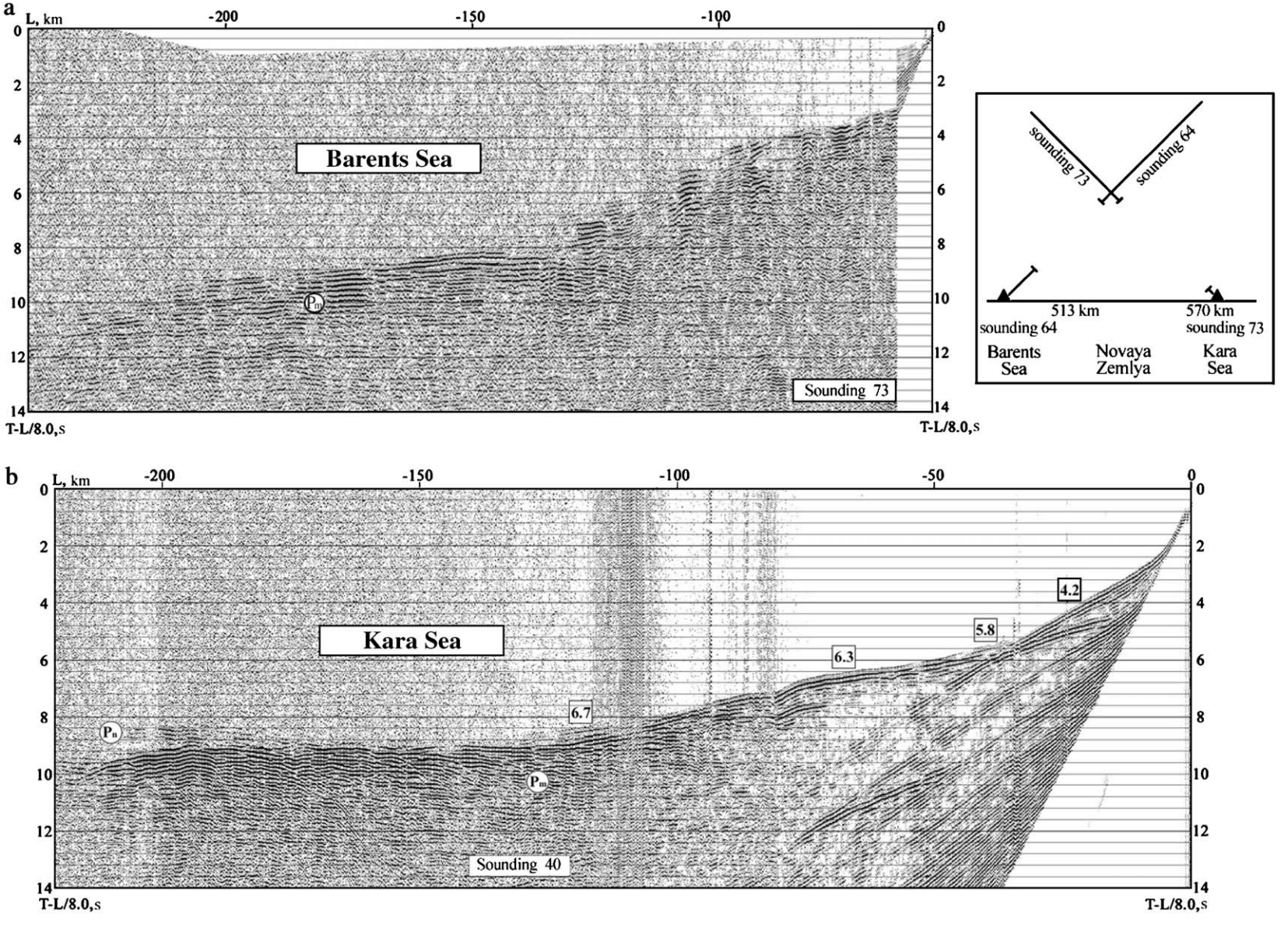

Fig. 3. Examples of wavefields: (a) Novozemelskiy segment of Line 2-AR, sounding 73, a line distance of 576 km; (b) Line 2-AR, Kara Sea, sounding 40, a line distance of 905 km. Reduction velocity 8 km s^{-1}. Values in squares — apparent velocities in km s^{-1}.

recorded at most stations, starting with offsets of 60–100 km (Figs. 2b and 3b). They are traced reliably up to offsets of 150–200 km, reaching in few cases offsets of 250–320 km. On the large offsets, the travel–time curves have the typical shape with apparent velocity V^* decreasing from values 9.0–10.0 km s^{-1} in the beginning of wave tracing down to values 6.5–7.5 km s^{-1}, according to V^* of the wave refracted in the overlaying layer. Near critical incidence, the Pm coda is frequently a complex interference signal from several waves.

The reflected wave from the Moho on 1-AR is reliably traced in the Kola-Kanin Monocline, and across Central Barents Zone of uplifts. There is a window in North-Barents Basin in the interval of 950–1080 km where the reflection from the Moho is practically absent (Fig. 2à, right branch). It is notable, that on 2-AR the reflected wave from Moho is not traced in the North-Barents Basin from 110 km up to 260 km.

It is particularly important to note the complicated character of reflected waves Pm in Kara Sea (Fig. 3b). The reflections from the Moho are strong. The Moho refractions (Pn) with $V^* = 7.8–8.5$ km s^{-1} are observed at few soundings and as first arrivals at offsets of 140–160 km for short intervals of 20–30 km (Fig. 3b).

2. The waves generated inside the crystalline crust, have apparent velocities of 6.5 to 7.0 km s^{-1} and start as first arrivals at offsets of 80 to 100 km. The waves are traced practically everywhere, but are weaker arrivals (Figs. 2b and 3b). They have a reflection like travel–time curve with gradually dropping apparent velocity and appear as first arrivals due to amplitude attenuation of the previous waves. At offsets of 140–160 km they are replaced as first arrivals by the refracted wave from the Moho.
3. Waves connected to the top part of the crystalline crust, are traced everywhere, but vary in amplitude. The origin of these waves (refracted or reflected) cannot always be determined unambiguously. Only on the southern part of line 1-AR (in the Kola-Kanin Monocline), clear refracted waves with an apparent velocity of 5.6–6.2 km s^{-1} characterized by parallel refraction time–distance curves from adjacent shot points (typical for this type of waves) appear as first arrivals at offsets 5–70 km. At larger offsets these arrivals are replaced by a lower amplitude wave with an apparent velocity of 6.0–6.4 km s^{-1} (Sakoulina et al., 2000).

   In the Central-Barents Zone of uplifts and North-Barents Basin, as a rule, low amplitude, rapidly attenuated reflected waves with apparent velocities of 5.8–6.3 km s^{-1} are connected to the top boundary of the consolidated crust (Fig. 2).

   On the Kara segment of line 2-AR, the recorded energy associated with the top part of the consolidated crust has a very complicated character, which may be due to diffractions and anomalous values of apparent velocity (Fig. 3b).
4. The principal wave from the sedimentary cover is the refracted wave with $V^* = 5.2–5.8$ km s^{-1} connected with Permian–Carboniferous carbonates. The energy appears as high amplitude first arrivals at offsets from 30 km up to 80 km. The wave is frequently seen as reflected second arrivals, which can be traced over intervals of 10–20 km (Fig. 2b).

   The refracted waves connected to the top part of the sedimentary cover, with apparent velocities from 2.6 km s^{-1} up to 5.0–5.2 km s^{-1} are common except on the southern part of Line 1-AR and the Novozemelskiy segment of line 2-AR, where the thickness of the sedimentary cover is sharply reduced. These arrivals that originate from horizons in the Jurassic–Permian basins, may be continuous for up to 60 km and include principal apparent velocities of 2.6–3.1 km s^{-1}, 3.4–3.8 km s^{-1}, 3.8–4.5 km s^{-1} and 4.6–5.0 km s^{-1} (Figs. 2 and 3b).

   In the North-Barents Basin at offsets up to 40–50 km, interfering, multiphase wave packages with high attenuation are observed. These records are probably connected with trappean formations in the upper part of the sedimentary cover.

   The record section from the Novozemelskiy segment of Line 2-AR has a very complicated and ambiguous character (Fig. 3a). The wave from the Moho is precisely traced and identified. The presence of the diffractions, the incoherent seismic events, and distortions and interruptions of travel–time curves prevent wave identification.

4.1.2. WARRP data processing

Seismic record processing was targeted at increasing resolution allowing more reliable wave separation. The standard procedures of amplitude control, band and reverse filtering were applied. The processed records were then used for kinematic analysis (i.e. wave arrival time study) using software tools developed in Sevmorgeo (Sakoulina et al., 2003). Kinematic analysis included picking and storing arrival times in the data bank, wave separation and composing travel–time curves for solving inverse problems.

Two interpretation models were applied: (1) the model consisting of thick layers with laterally varying

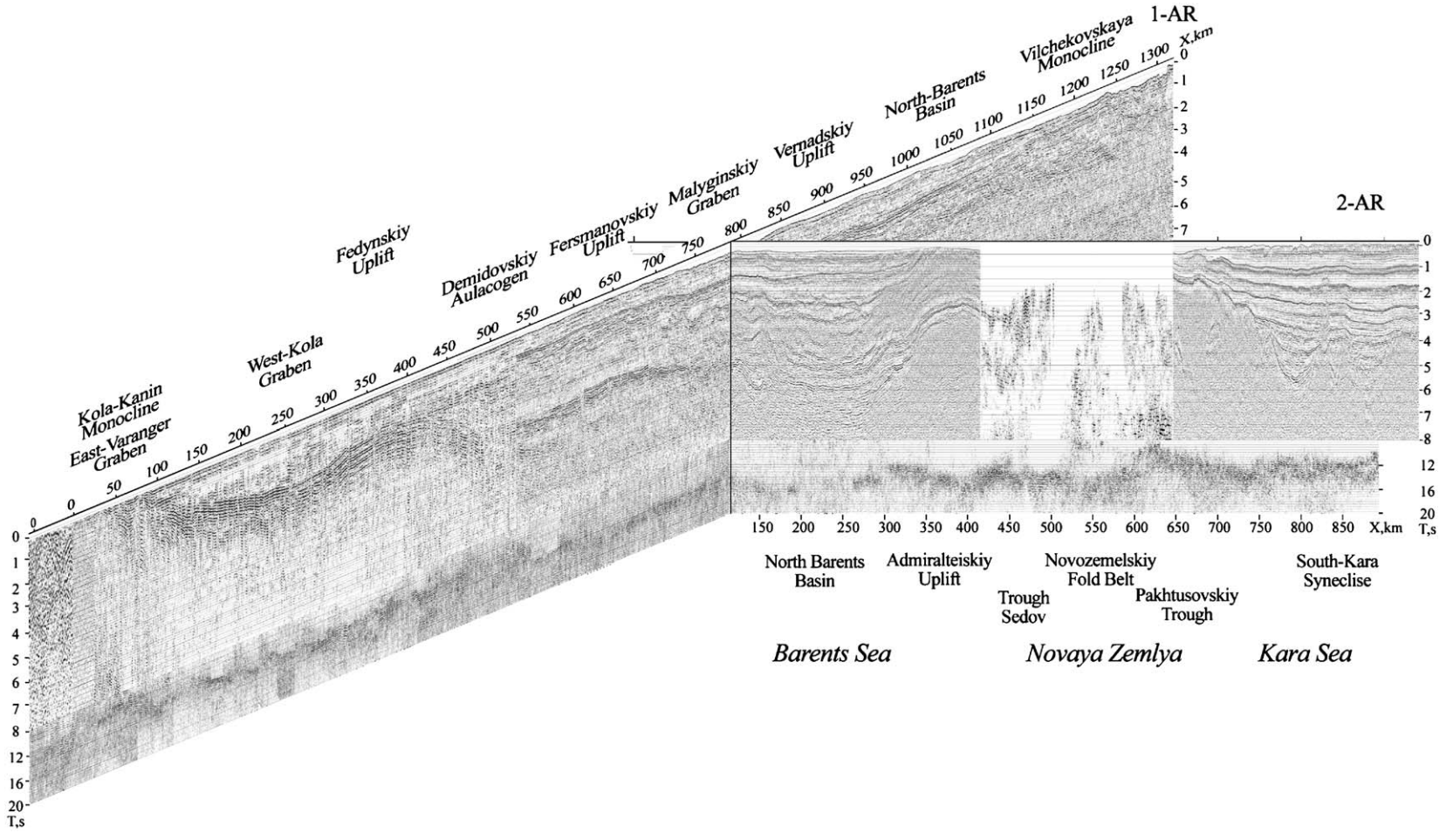

Fig. 4. Composite dynamic time sections on Line 1-AR and Line 2-AR: CDP section in the 0–8 s time interval; mid- point transformation of WARRP data in the 8–20 s time interval.

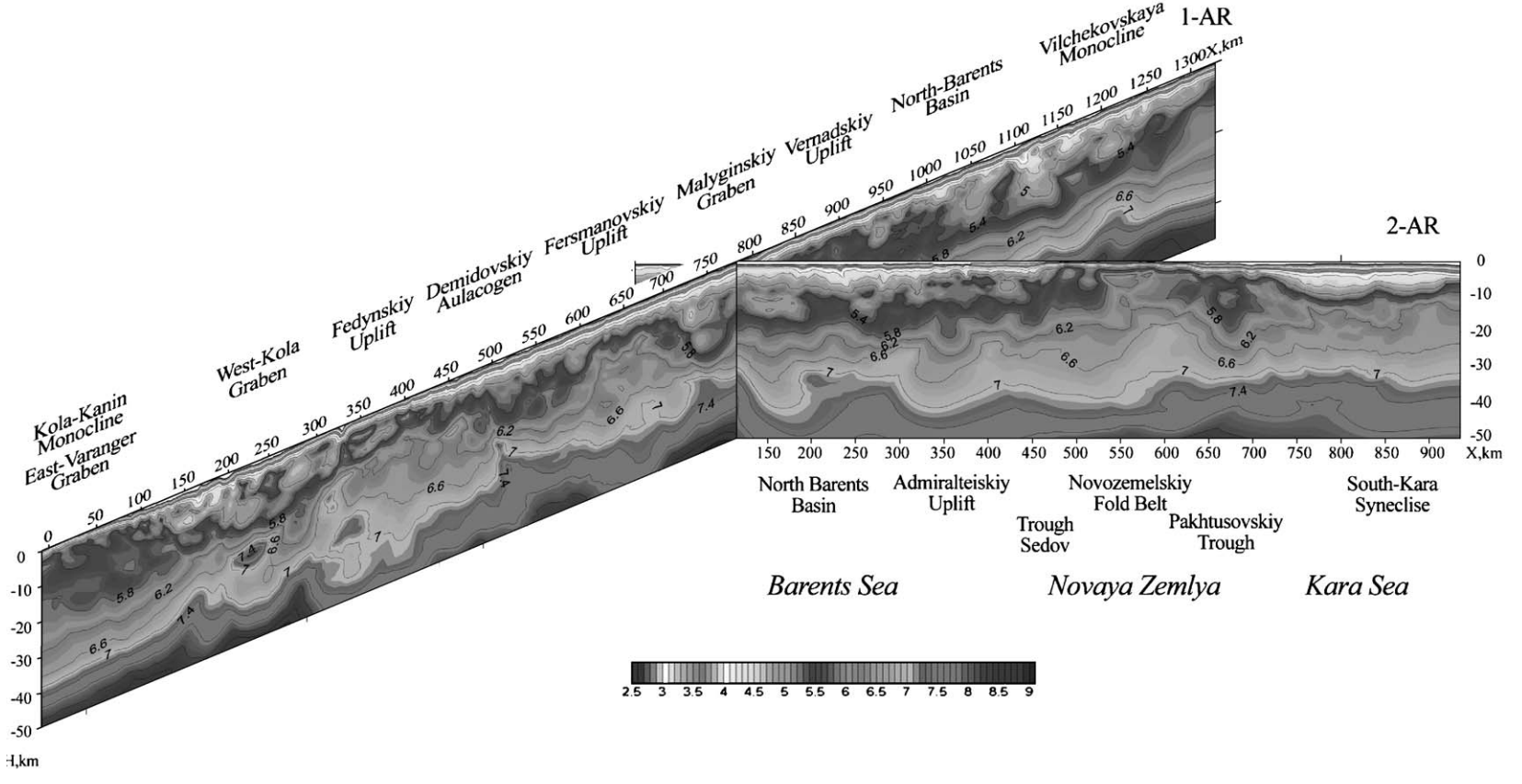

Fig. 5. Velocity models of the crust on Line 1-AR and Line 2-AR derived from first arrivals by the seismic tomography method.

velocities, and (2) the model of a continuous velocity distribution $V(x, z)$. Data for model (1) include reflection and refraction travel–time curves. Travel–time curve inversion produced the cross sections comprising the main horizons in sedimentary cover and crystalline crust. Data for model (2) include first arrivals for tomographic inversion. The software implements the technique partly described in Physics of the Solid Earth (Sakoulina et al., 2003).

Strong reflections from the Moho allowed building the Moho image and including it, along with CDP section, into the combined section image.

Application of all approaches has allowed extracting of maximum information from the WARRP data acquired.

4.2. MCS data

MCS data were processed in the PROMAX system. Various processing stages involved the multiple applications of deconvolution, single-channel bandpass filtering, multichannel *f–k* filtering and DMO procedures. Poststack migration was performed using the Kirchhoff algorithm. The time and depth sections formed the upper part in the combined section image.

4.3. Results of processing seismic data

Combining the results of MCS and WARRP data processing produced the general section images along the lines 1-AR and 2-AR in time and depth scales. In the 0–8 s time interval (accordingly in the 0–25 km depth interval) uses MCS data and in the 8–20 s time interval (accordingly in the 25–50 km depth interval) uses WARRP data, including, in particular, the reflection from the Moho. Joint representation of profiles 1-AR and 2-AR testify to the good matching of sections at intersections and enables volumetric depth model of the Barents–Kara region (Fig. 4).

The results achieved on lines 2-AR and 1-AR demonstrate advantages of integrating MSC and WARRP for studying crustal structure. MCS data provide detailed reconstruction of sedimentary cover with continuous tracing of internal boundaries, while WARRP data supply the velocity model of the whole section and the geometry of the basement and deep boundaries in the crystalline crust, including the Moho discontinuity. This integrated seismic model depicts the general layering and block structure of the crust and results in reliable geological cross-sections.

The tomographically derived velocity models of the crust for lines 1-AR and 2-AR are jointly represented in Fig. 5. Taking into account relative independence of both sets of the initial data, and the results of tomographic processing, confidence in the final model is supported by the matching of models at the profile intersection.

All major structures crossed by lines, were precisely displayed on tomographic sections. It is necessary to emphasize especially, that tomographic processing on Line 2-AR has allowed the first velocity model of the Novozemelskiy Fold Belt. In addition, a low-velocity anomaly at a depth of 10 km in the western part of Kara Sea (650–680 km) was very distinctly located. This anomaly corresponds to western board of the Pakhtusovskiy Trough, which appears on CDP section.

5. Results

The basic result of investigations was the construction of geological model of a deep structure Earth's crust on the basis of complex seismic interpretation of MCS, WARRP data and geologic–geophysical data. As a result the full section of Earth crust with basic crust's boundaries and horizons in sedimentary cover, have been composed (Fig. 6).

The results obtained in the southern part of Line 1-AR (1995) were presented in (Verba et al., 1998, 1999; Sakoulina et al., 2000, 2003). Preliminary results for all profile 1-AR were discussed in EAGE Conferences (Ivanova et al., 2001; Ivanova, 2003).

Four main tectono-stratigraphic units are distinguished in the section of the Earth's crust: (1) a sedimentary cover; (2) the Upper Proterozoic (mainly Riphean for the Barents Plate) and Riphean–Paleozoic (the South-Kara Syneclise) deformed and folded complexes; (3) the upper crystalline crust (granite-gneissic metamorphic Archean–Proterozoic complex); (4) the lower crust (basalt complex).

5.1. Deep structure

The crustal structure of the Barents–Kara Region on regional lines 1-AR and 2-AR is shown in Fig. 6. The Barents–Kara Region is characterized by reduced continental and subcontinental crust with the average thickness of 37–39 km. On islands and areas of uplifts with ancient massifs, the thickness of the crust (38–42 km) approaches the typical crust for a continental platform. Within the Novozemelskiy Fold Belt the thickness of the crust reaches 40–42 km. Rift-related grabens are characterized by 33–36 km-thick crust. At the base of the crust, the Moho is traceable as a reflector/refractor with a boundary velocity of 7.9–8.1 km s^{-1}. Within the North-Barents Basin and Noyabr'skiy,

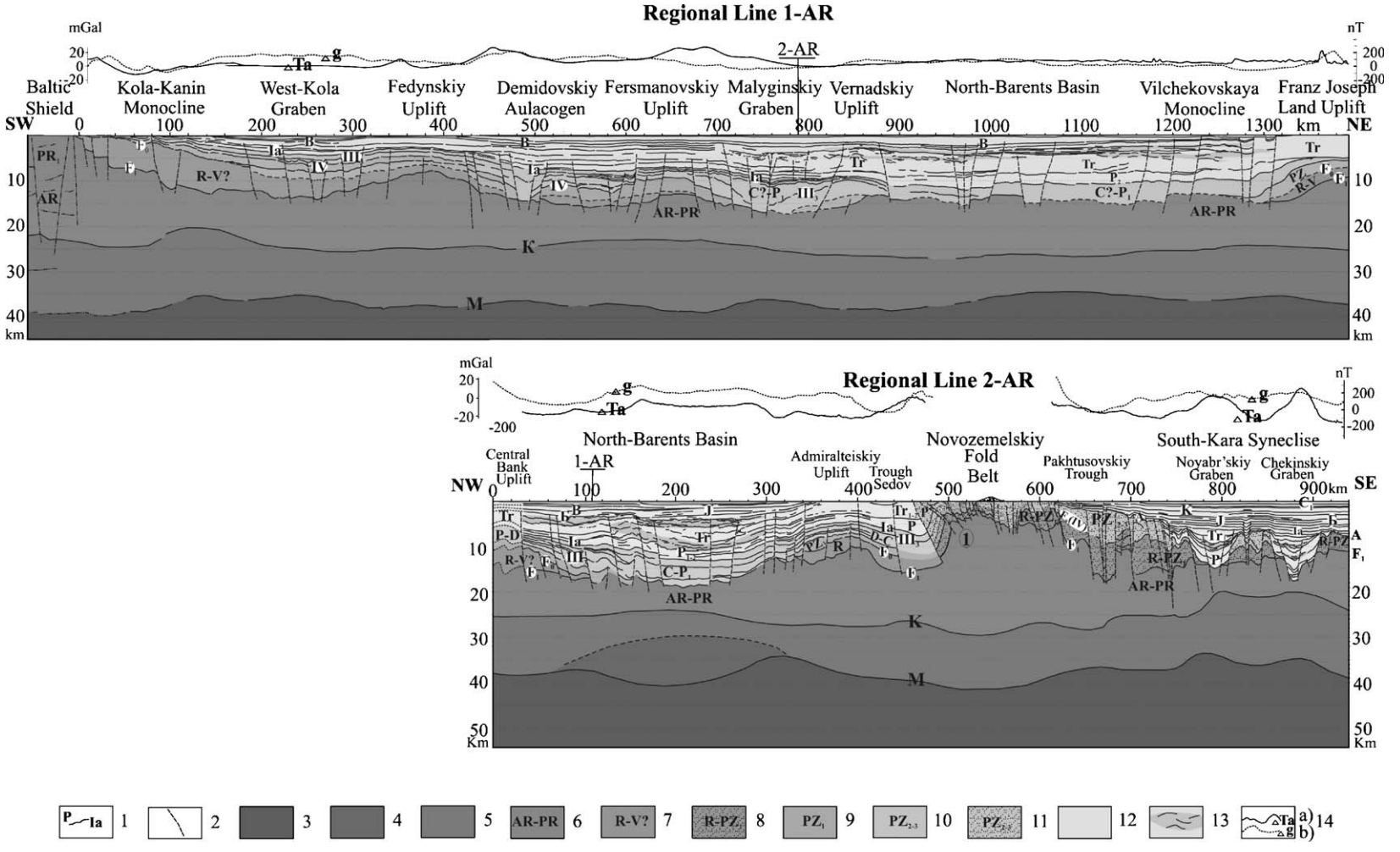

Fig. 6. Geological–geophysical sections of the Earth's crust along regional lines 1-AR and 2-AR (the Barents–Kara Region). 1, Seismic Horizon, its index and stratigraphy; 2, main faults (circled number-1 on Line 2-AR, Main Novozemelskiy Fault); 3, Upper Mantle; 4, Crust–Mantle mixture, 5, Lower consolidated crust; 6, Upper consolidated crust (AR-PR); 7, Riphean complex (R-V?), 8, Riphean–Lower Paleozoic deformed complex ($R\text{-}PZ_1$); 9, Lower Paleozoic terrigenous–carbonate complex (PZ_1); 10, Middle–Upper Paleozoic terrigenous carbonate complex; 11, Middle–Upper Paleozoic deformed complex (PZ_{2-3}); 12, Upper Paleozoic–Mesozoic terrigenous complex; 13, high velocity volcanic-terrigenous layers in sedimentary cover; 14, curves of: (a) magnetic anomalies, (b) gravity anomalies.

Chekinskiy graben structures, large uplifts (mantle "dome") are fixed by the Moho boundary. Based on integrated interpretation of seismic data, a lens of crust–mantle mixture is distinguished in the North-Barents Basin (Fig. 6). The lower crust thickness varies from 5 to 19 km, significantly decreasing to 5–10 km on the flanks of the North-Barents Basin, and increases within the South-Kara Syneclise. The mid-crust boundary (K) is recognized at depths of 20–30 km with maximum depths 27–30 km within the Novozemelskiy Fold Belt and minimum depths 20–22 km in the deepest part of the South-Kara Syneclise (the Noyabr'skiy and Chekinskiy grabens). The K boundary velocities are stable, at about 6.8–7.0 km s^{-1}.

The thickness of the upper crust varies considerably from 3–8 km in grabens to 15–20 km within the Baltic Shield and Fedynskiy Uplift, and 20–25 km beneath the Admiralteiskiy Uplift and Novozemelskiy Fold Belt. The upper crust forms consolidated crystalline basement, represented by metamorphic and intrusive rocks of Archean–Proterozoic age. In Fig. 6 the F_1 surface, with refraction velocities 6.0–6.6 km s^{-1}, is identified as the top of granite-gneissic basement. Within the Kola-Kanin Monocline, based on a well tie to the superdeep borehole (SD-3) on the Kola Peninsula, the F_1 surface, with the refraction velocity 6.1–6.6 km s^{-1}, is identified as the top of metamorphosed volcanic-sedimentary rocks of the Lower Proterozoic Pechenga Series, found in SD-3 at a depth of 6.8 km s^{-1} (Verba et al., 1998). Outcroppings of the Lower Riphean are mapped on the Island Severny of the Novaya Zemlya Archipelago and are represented by metamorphic rocks (marbles, quartzites, crystalline schist, gneiss). In spite of the paraplatform character of these deposits, they are considered basement complexes, since the Novaya Zemlya deposits are folded and metamorphosed (Korago et al., 1992).

The Upper Proterozoic section within most of the Barents Plate includes mainly Riphean subplatform sediments and, in place, Vendian terrigenous deposits. Vendian metamorphic rocks with inclusions of dolerites are revealed in the Nagurskaya hole on the Archipelago Frantz Joseph Land (Gramberg et al., 1988). The F_0 surface, with a refraction velocity 5.7–5.9 km s^{-1}, generally corresponds to the top of the Upper Proterozoic (Riphean) rocks. These rocks crop out on the Sredniy and Rybachiy peninsulas and on Kildin Island (Rybachinskaya, Kildinskay and Volokolovskaya Series) and are composed of dolomites, limestones, sandstones, siltstones and argillites. The F_0 surface is the most important boundary in the section and separates the non-fold complexes of the sedimentary cover from the denser, underlying deformed complexes. The thickness of Riphean deposits may be as much as 5–9 km, increasing to 12–13 km within the graben structures, revealed on the Kola-Kanin Shelf (Verba et al., 1998; Ivanova, 2001). The Riphean deformed complex with maximum thickness 2.5–5.0 km is distinguished within the large uplifts (the Fedynskiy, Fersmanovskiy, Central Barents, Franz Joseph Land, Admiralteiskiy). The Riphean–Lower Paleozoic low-metamorphic complex with velocities 5.8–6.0 km s^{-1} is distinguished between surfaces F_1 and F_0 (IV) within the Novozemelskiy Fold Belt, Pakhtusovskiy Trough and most of the South-Kara Syneclise except the rift grabens (the Noyabr'skiy, Chekinskiy). Geological data on the northern geo-block of Novaya Zemlya indicate that the Upper Proterozoic flyschoid aspid deposits together with overlying Early Paleozoic–Silurian deep-water and shallow-water molassoid deposits form united structural-material complex (Korago et al., 1992). The overlying Middle–Upper Paleozoic folded complex is traced between surfaces F_0 (IV) and A and has a maximum thickness of 5–6 km in the Pakhtusovskiy Trough (Figs. 6 and 7). The complex is characterized by the boundary velocities 5.1–5.6 km s^{-1}. In Fig. 7 the MCS section shows the top of this complex acoustic basement (the surface A). By analogy with the Novozemelskiy geological section, the complex may be represented by terrigenous–carbonate deposits of Silurian–Devonian, deep-water cherty-clayey of Lower Carboniferous and Upper Paleozoic argillites (Korago et al., 1992).

5.2. Sedimentary cover

Three major tectono-sedimentary complexes are distinguished in the sedimentary cover of the Barents Plate: a lower terrigenous–carbonate complex of Early Paleozoic age, a middle terrigenous–carbonate complex of Middle-Late Paleozoic (Devonian–Permian) age and an upper terrigenous complex of Late Permian–Cenozoic age.

The lower terrigenous–carbonate complex includes terrigenous and carbonate rocks from the Cambrian to Silurian. Horizon IV is associated with the Silurian carbonates. The complex is characterized by small deformations caused by Caledonian tectogenesis especially within the Fedynskiy and Fersmanovskiy uplifts (Fig. 8). The complex is significantly affected by faulting. The complex which developed in the southern, central and eastern parts of the Barents Plate, appears to terminate at the southern part of the Kola-Kanin Monocline and is not represented in the South-Barents

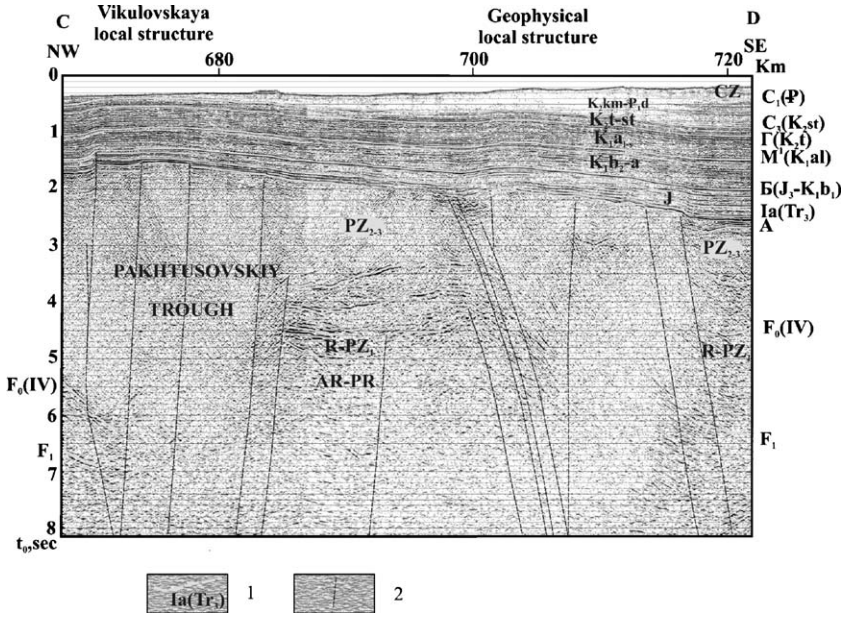

Fig. 7. Fragment of the MCS Line 2-AR, illustrating Pakhtusovskiy Trough (the western part of the Kara Shelf). 1, Seismic Horizon, its index and stratigraphy: C_1 — bottom Paleogene, C_3 — top Santonian (K_2), Г — bottom Turonian (K_2), M^1 — bottom Albian (K_1), Б — lower part of the Lower Cretaceous, Ia — bottom Jurassic, A — surface of acoustic basement, top of deformed Upper–Middle Paleozoic complex, F_0(IV) — top of Riphean–Lower Paleozoic deformed complex, F_1 — top of Archean–Proterozoic consolidated basement; 2, main faults.

and the North-Barents basins. The overall thickness of the Early Paleozoic terrigenous–carbonate complex is estimated to be 0.5–3.5 km with maximum thickness within the West-Kola Graben.

The middle-upper Paleozoic terrigenous–carbonate complex (Devonian–Permian) includes the Devonian and Carboniferous–Permian units. The Devonian unit is mainly terrigenous sediments, with carbonate rocks in

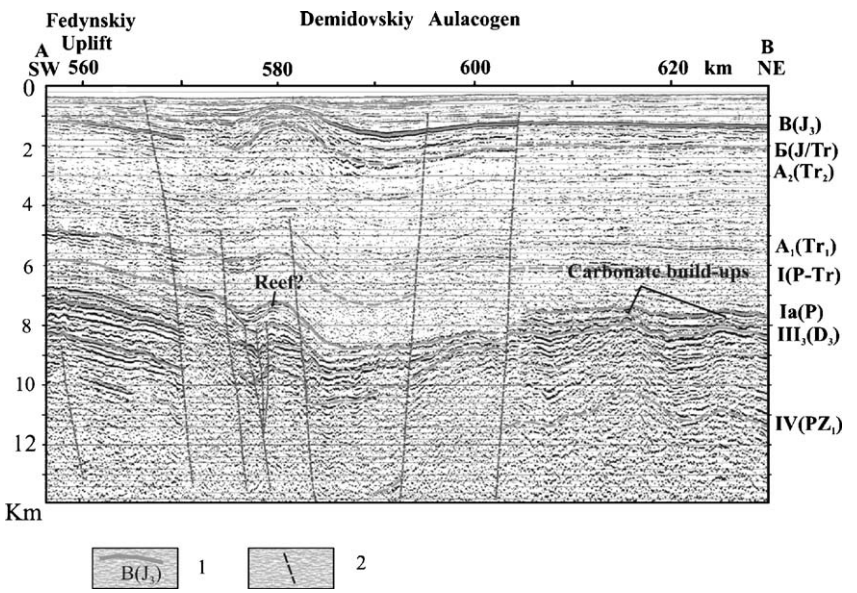

Fig. 8. Fragment of the MCS Line 1-AR, illustrating an anticlinal structure in the junction zone of the Fedynskiy Uplift and Demidovskiy Aulacogen. 1, Seismic Horizon, its index and stratigraphy: B — top Upper Jurassic, Б — top Upper Triassic, A_2 — Middle Triassic, A_1 — Lower Triassic, Ia — top Permian carbonates, III_3 — Upper Devonian, IV — top Silurian; 2, main faults.

the upper part of the section. Bands of tuff and basalt may be present especially in rift grabens. The top of the unit corresponds to seismic Horizon III_3 (D_3). The Devonian section is affected by anticlinal folding, especially within the southern slope of the Kola-Kanin Monocline and zone of junction rift grabens and uplifts (Fig. 8). Devonian deposits vary considerably in thickness and lateral extent. The Devonian unit is not clearly distinguished in the North-Barents Basin. The thickness of the Devonian unit varies from 0.25 to 5 km, with maximum thickness in the Demidovskiy Aulacogen. Based on the similarity between the Devonian section of the Demidovskiy Aulacogen and synchronous sections of the Pechora Syneclise (Pechoro-Kolvinskiy Aulacogen) and West-Spitsbergen graben, Verba et al. (1998) suggest that these sections were formed in a common riftogenic paleo-graben. The Carboniferous–Permian carbonate unit represents the upper part of the Middle–Upper Paleozoic complex and is represented by sandy-clayey deposits with anhydride inclusions in the lower part and mainly carbonates with evaporates in the upper part. This upper part forms a Late Carboniferous–Permian carbonate platform, which is widely developed in the southern, central and eastern parts of the Barents Plate except the deepest parts of the South-Barents and North-Barents basins. Horizon Ia, with boundary velocities 4.8–5.6 km s^{-1}, represents the top of Permian–Upper Carboniferous carbonates. Horizon Ia is diachronous, younging from Early Permian to Late Permian. A facies transition of shelf carbonates to deep-water clayey deposits took place on the flanks of the South-Barents and North-Barents basins. Subsidence of the carbonate platform is fixed within large fault zones, forming the North-Barents and South-Barents basin. Traced in the base of the sedimentary cover, the Carboniferous–Lower Permian volcanic-sedimentary unit is characterized by high velocities 5.8–6.2 km s^{-1} within the North-Barents Basin. The overall thickness of the terrigenous–carbonate Devonian–Permian complex varies from 1–2.5 km on the Kola-Kanin Monocline and uplifts to 3–5 km in the Demidovskiy Aulacogen, Malyginskiy Graben and North-Barents Basin.

The Late Permian–Cenozoic upper terrigenous complex comprises clastic deposits mainly of Late Permian–Early Cretaceous age. It is not present throughout the Barents Plate, being eroded to the south, north and on large uplifts especially within the Fedynskiy and Admiralteyskiy uplifts. The Upper Permian–Triassic unit forms the main part of this complex. The lower part of the unit is characterized by clinoform structures, dipping to the northeast on the Kola-Kanin Monocline and to west on the eastern flank of the North-Barents and South-Kara basins. The thickness of the Upper-Permian–Triassic unit varies from 1.7 to 2.7 km in the Kola-Kanin Monocline, 2.5–3.5 km within Fedynskiy Uplift, 4.0–5.5 km in Demidovskiy Aulacogen and Admiralteyskiy Uplift, and reaches 10–12 km in the North-Barents Basin. At the top of the Triassic unit is Horizon Б (J/T), representing the Pre-Jurassic unconformity surface. Triassic rocks are represented by rhythmical alternation of sand-shale deposits, with coals in the upper part of each cycle. Seismic data (intensive irregular high-velocity reflectors) testify to a presence of vulcanites in the form of layer intrusions (trappean formation) and stocks in the Upper Permian and Triassic section within the North-Barents and South-Barents basins (Figs. 4, 6 and 9)). The Jurassic–Cenozoic unit is represented across the whole Barents Region. The thickness of this unit gradually increases from 100–200 m on the periphery of the Barents Plate to 2.5–3.5 km in grabens and basins. The Jurassic unit is composed of sand-shale deposits. Seismic Horizon B corresponds to clay at the top of the Upper Jurassic section.

Three major undeformed structural–formational complexes are distinguished in the sedimentary cover of the South-Kara Syneclise: a rift terrigenous complex of Late Paleozoic–Triassic age, structural complexes of Jurassic–Paleogene age and Pliocene–Quaternary.

The Upper Paleozoic–Triassic complex is mainly terrigenous and occurs between Horizon A and Ia (Figs. 6, 7). Horizon A is connected with the base of non-deformed sedimentary cover. Horizon A reflects fault-block structure of the Paleozoic deposits deformed in various degrees by Hercynian and Early Cimmerian tectogenesis. Horizon Ia is associated with the top of Triassic deposits. From seismic records (strong reflectors), gravity and magnetic data, effusive rocks are expected to be a part of the lower complex (Figs. 4 and 6). The lower complex forms a rift (taphrogenous) cover and is located only within graben-like basins. The maximum thickness (7–9 km) of this complex is determined in the Noyabr'skiy and Chekinskiy grabens. The velocities vary from 5.3–6.0 in the lower section of the complex to 4.0–4.7 in the upper section.

The post-rift Jurassic–Paleogene complex is represented by several rhythmic–stratigraphic cycles, with conforming dips. Every cycle consists of a transgressive part of marine clayey sediments (source rocks and cap rock) and aleurolite-sand, coarse sand and coal-bearing facies (reservoirs). Two major units are distinguished in the Jurassic–Paleogene complex. They are: 1 — the Jurassic–Lower Berriasian (between Horizon Ia and Б, Fig. 7) an argillite–aleurolite–sandy formation with

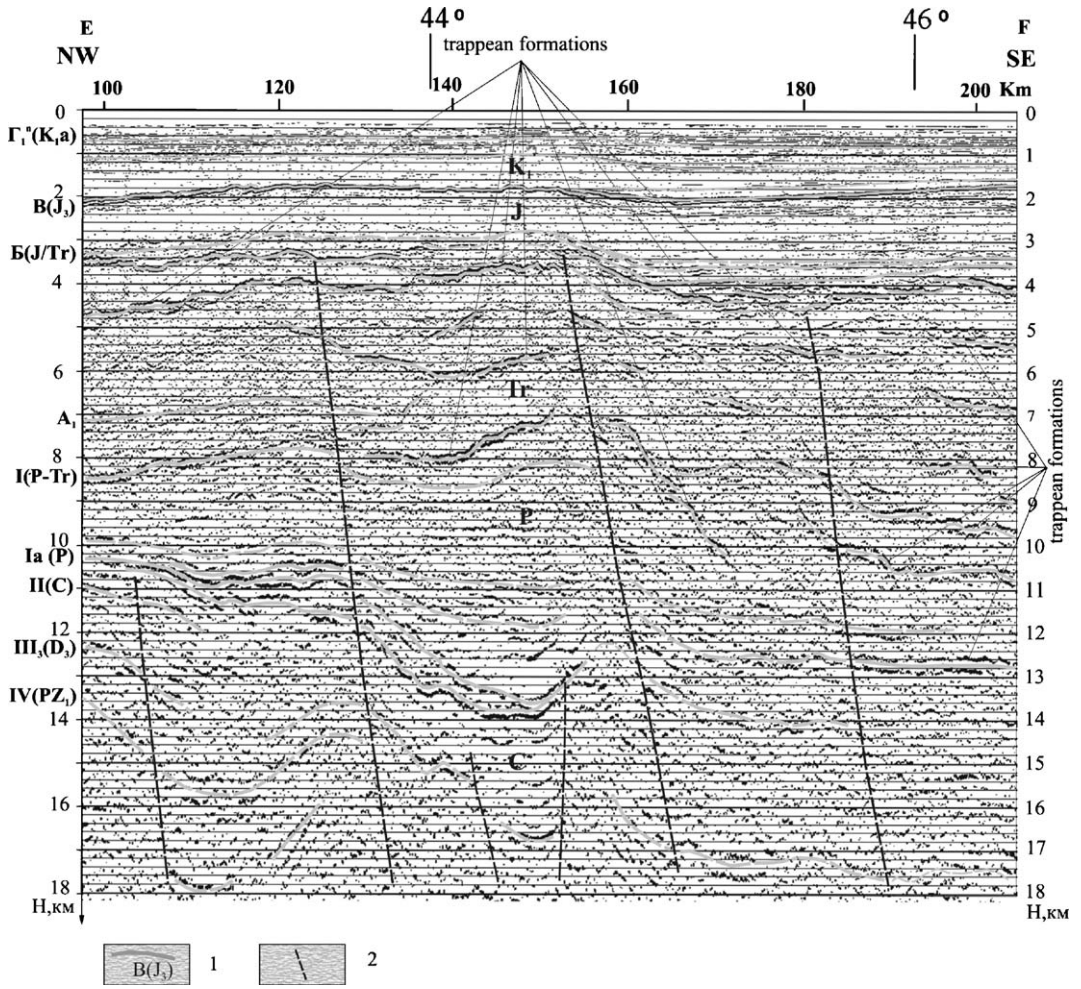

Fig. 9. Fragment of the MCS Line 2-AR, illustrating presence trappean formations within the southwestern part of the North-Barents Basin. 1, Seismic Horizon, its index and stratigraphy: $Г_1^n$ — aptian, В — top Upper Jurassic, Б — top Upper Triassic, A_1 — Lower Triassic, Ia — top Permian carbonates, II — lower part of the Carboniferous, III_3 — Upper Devonian, IV — top Silurian; 2, main faults.

mainly clayey rocks including bituminous shales in the upper part, with a thickness of 2.0–2.5 km and velocities that vary from 4.2–4.4 km s^{-1} in lower part to 3.5–3.7 km s^{-1} in upper part; 2 — the Cretaceous–Paleogene unit of sandy–clayey–aleurite formation with maximum thickness 3.5 km in grabens, velocities increases with the depth from 3.3–3.6 to 2.0–2.2 km s^{-1}.

The Pliocene–Quaternary complex, represented by glacial-marine sediments with an average thickness 50–100 m, lies with angular and stratigraphic unconformity on eroded Mesozoic–Cenozoic strata.

6. Conclusions

Deep seismic investigations along regional lines 1-AR and 2-AR specify the deep structure of the Earth's crust of the Barents–Kara Region (Fig. 6). The advanced equipment and high density of observations used in the WARRP have increased the accuracy of deep seismic results. Observations on lines 1-AR and 2-AR demonstrate the effectiveness of integrating the WARRP with OBS and reflection-MCS methods for studying the geological structure of the crust. Reflection-MCS observations are optimal for the study of the sedimentary cover, enabling the continuous tracing of its boundaries and, where possible, the basement. WARRP provides information on the basement and deep boundaries in the crust, including the Moho, as well as the crustal velocity structure.

New seismic data provide constraints on the deep structure of main tectonic elements of the Barents–Kara Region. Several grabens are revealed: the Riphean Graben on the Kola-Kanin Monocline,

Lower Paleozoic West-Kola Graben, Devonian Demidovskiy Aulacogen, Malyginskiy Graben in the Barents Region and Noyabr'skiy and Chekinskiy grabens in the Kara Region. Riphean grabens are developed in the southern part of the Barents Shelf along the Kola Peninsula and in the northern part of the White Sea trending SE to the western slope of the Kanin–Timanskiy Fold Belt (Ivanova, 2001). To the northwest, the West-Kola Graben is established in the relief of the basement and in Lower Paleozoic part of the sedimentary cover. The West-Kola Graben is filled with the Lower Paleozoic synrift complex of sediments with the thickness of 2.5 to 3.5 km. Large grabens are revealed in the central part of the Barents Plate — the Demidovskiy Aulacogen and Malyginskiy Graben (Figs. 1 and 6). The central graben of the Demidovskiy Aulacogen is filled with 3–5 km of Devonian synrift sediments, whereas the base of the Malyginskiy graben is suspected to have a 7 km thick layer of Carboniferous–Lower Permian synrift sediments. Grabens are strongly affected by NW–SE trending fault zones. To the northeast and east of the grabens mentioned earlier, a vast zone of rift graben (the North-Barents Basin) is revealed where mainly the Upper Paleozoic–Mesozoic terrigenous sediments form the sedimentary cover. The lines 1-AR and 2-AR reflect mainly the eastern and southern part of this basin. Here, the base of the sedimentary cover is thought to contain sediments from the Carboniferous–Lower Permian terrigenous–volcanic complex. It is considered evidence of an initial stage of developing rift in the North-Barents Basin. The large thickness of the Upper Permian–Triassic terrigenous sediments (10–12 km), containing significant quantities of magmatic bodies (intrusive and effusive rocks), is interpreted as evidence for a main phase of rifting in Upper Permian–Triassic time.

Throughout the Permian–Triassic, the Barents–Kara Region experienced a significant period of development. From early Permian to late Permian, the composition of deposits changed from carbonate–terrigenous to exclusively terrigenous. Meanwhile, the sedimentation rate was increased very rapidly especially in the South-Barents and North-Barents basins and South-Kara Syneclise. During the late Permian–Triassic, the activation of destructive processes in the Barents-Kara Region occurred simultaneously with an initial stage of the opening of the Arctic Ocean (Pogrebitsky, 1997), suggesting a geodynamical connection between the two events.

The deep structure of the Earth's crust is first studied in the South-Kara Syneclise, where it is complicated by the large rift-grabens, Noyabr'skiy and Chekinskiy, that contain up to 15–17 km of sedimentary cover. Along line 2-AR, grabens are relatively symmetrical; in the western part of the South-Kara Syneclise, a graben-like structure with a sedimentary cover 8–9 km deep is revealed (740–760 km on line 2-AR in Fig. 6). Rift complex of Late Paleozoic (mainly Permian)–Triassic age and is represented by terrigenous with volcanic rocks with a thickness estimated to be 4–9 km.

By integration of WARRP and MCS, a large structural element – the Pakhtusovskiy Trough – has been identified in the western part of the Kara Shelf (Figs. 6 and 7). It is filled with deformed Riphean and Paleozoic deposits forming transitional structure between consolidated Archean–Proterozoic basement and non-dislocated terrigenous cover having mainly Mesozoic age. The total thickness of Paleozoic and Riphean deformed terrigenous molassoid carbonate deposits reach 9–12 km. The Pakhtusovskiy Trough is limited by faults displacements of 1.5–2.5 km.

For the first time the deep structure of the Novozemelskiy Fold Belt has been studied by deep seismic investigation along line 2-AR. A velocity image from the seismic tomography model (Fig. 5, km 460–570 on the line 2-AR) emphasizes the collisional character of the Novozemelskiy Fold Belt. As a result, more ancient folded rocks of the Novozemelskiy Fold Belt superpose non-folded complexes of the sedimentary cover the Trough Sedov. Figs. 5 and 6 at 460–480 km on line 2-AR, show the advanced front of the thrust belt complicating the east board of the Trough Sedov. To the east, a tomographic study of the regional Main Novozemelskiy Fault (Korago et al., 1992) at 500 km of Line 2-AR (Figs. 5 and 6) reveals a low velocity area (isolines 5.0–5.5 km s^{-1}), which suggests a zone of decompression as deep as 10–11 km (Fig. 5).

The main features of the deep structure Barents–Kara Region are: (1) the collision character of the junction zone of the Barents Plate and West-Siberian Plate; (2) graben structures in the section of the sedimentary cover and basement; (3) the disjunctive character of graben and presence of listric faults; (4) extremely large thickness of sedimentary cover estimated as 14–18 km; (5) a presence in the bottom of the grabens of thick high velocity (velocities up to 5.6–6.2 km/s) series of volcanic-sedimentary rocks; (6) a presence of trappean formations, located mostly in the Upper Paleozoic and Triassic part of the section; (7) reduced thickness of the granite-gneissic complex to 3–8 km and Earth's crust to 33–36 km in grabens; (8) a presence of the mantle "domes", largest of them is fixed within

Noyabr'skiy graben and the eastern slope of the North-Barents Basin. These features are connected with processes of epicontinental riftogenesis, earlier assumed by Verba, 1985; Gramberg, 1997. From the data on the deep structure, we conclude that mainly destructive processes contributed to the dynamics of forming the Barents–Kara Region. Several rift complexes are distinguished in sedimentary cover: the Riphean, Lower Paleozoic, Devonian, Upper Paleozoic (Carboniferous–Lower Permian), and Upper Paleozoic (Upper Permian)–Triassic. The presence of an uninterrupted lateral series of rift complexes testifies to continuous spreading processes in the crust from Riphean to Triassic.

The rifting created tilted fault-blocks, which can be the significant petroleum traps, and the grabens with restricted marine conditions can host the deposition of source-rocks. Taking into account the rift character of main basins and grabens, the most pronounced structures generally occur at the uplifted edges of the grabens, associated with large fault zone. Fig. 8 illustrates a large structure in the junction zone of the Fedynskiy Uplift and Demidovskiy Aulacogen.

This investigation into the deep structure of the Earth's crust indicates, that the Barents–Kara Region is mainly characterized by a continental-type crust that narrows in certain regions from south to north (up to 40–35 km, Fig. 6). All detected rift-grabens are characterized by thinner crust and the presence of Mantle "domes" beneath them. The observed lens of a crust–mantle mixture within the North-Barents Basin appears to be connected with destruction of continental crust. One result of this destruction is the rising of melted material from mantle to the lower part of crust, creating a conversion of lower layers and/or replacement of the continental crust with mantle material.

Acknowledgements

The authors would like to thanks SEVMORGEO for their contribution and permission to use their seismic data and publish this work. Authors are very grateful to Chuck Hurich (Guest Editor — Tectonophysics) and reviews Dave Forsyth and Trine Dahl-Jonson for useful comments and again Dave Forsyth for his editing of the English text.

References

Fedorovckiy, Ju.F., Tronov, Ju.A., Vinnikovskiy, V.S., Evsukov, V.T., Tanygin, I.A., Zalivchiy, O.A., 1993. Significant results prospecting/exploring works in the Barents–Kara Region. Geodynamic and Oil–Gas Potential in the Arctic Region. Nedra, Moscow, pp. 15–19 (in Russia).

Gramberg, I.S., 1997. The Barents Permian–Triassic paleorift and its importance for a problem of the oil and gas potential of the Barents–Kara Plate. DAS (Reports of Academy Science) 352 (6), 789–791.

Gramberg, I.S., 1988. In: Alekhin, S.V., Baturin, D.G., Bro, E.G., Verba, V.V., Verba, M.L., Vinogradov, A.V., Volk, V.E., Gurevich, V.I., Daragan-Susheva, L.A., Zhuravlev, V.A., Ivanova, N.M., Krasilschikov, A.A., Malovictkiy, Ya.P., Pchelina, T.M., Ronkina, Z.Z., Shipilov, Ed.V., Yunov, A.Yu., Yashin, D.C. (Eds.), Barents Shelf Plate. Nedra, Leningrad. 263 pp. (in Russian).

Ivanova, N.M., 1997. Prospective Palaeozoic reefs in the southern part of the Barents Sea Shelf. Petroleum Geoscience, vol. 3, pp. 153–160.

Ivanova, N.M., 1998. Tectonic setting, stratigraphy, and petroleum potential of the South-Kara Syneclise. Extended Abstract. 60th Conference and Technical Exhibition, vol. 2. European Association of Geoscientist and Engineers, Leipzig, Germany, p. 544.

Ivanova, N.M., 2001. The geological structure and petroleum potential of the Kola-Kanin Monocline, Russian Barents Sea. Petroleum Geoscience, vol. 7, pp. 343–350.

Ivanova, N.M., 2003. Main Petroleum objects of the central part the Barents Region from seismic investigation. Extended Abstract. 65th Conference and Technical Exhibition, vol. 2. European Association of Geoscientist and Engineers, Stavanger, Norway, p. 162.

Ivanova, N.M., Kavoun, M.M., 1996. Main geological results within geotransects—the Island Vaigatch–Severnya Zemlya, the Yamal–Edgeoya. Extended Abstract. 58th Conference and Technical Exhibition, Amsterdam '96, vol. 2. European Association of Geoscientist and Engineers, The Netherlands, p. 572.

Ivanova, N.M., Matveev, Yu.I, Verba, M.L., 2001. Deep structure of the Barents Plate from geophysical investigation. Extended Abstract. 63th Conference and Technical Exhibition, vol. 2. European Association of Geoscientist and Engineers, Amsterdam, The Netherlands, p. 025.

Korago, Ev.A., Kovaleva, G.N., Il'in, L.G., Pogrebitskiy, Ul.EV. (Eds.), 1992. Tectonic and Metallogeny of Early Cimmerid of the Novaya Zemlya. Nedra, St. Petersburg. 195 pp. (in Russian).

Kunin, N.Ya., Joganson, L.I., 1982. Geophysical description and structure of the Earth's crust of the West Siberia. Bulletin of the Moscow Naturalist Society, Geological Section, vol. 61. Part 6 (in Russian).

Pogrebitsky, Yu.Ye., 1997. Opening of the North-Arctic Ocean and existing geological processes on surrounding continents. Regional Geology and Metallogeny, vol. 7, pp. 129–136 (In Russian).

Sakoulina, T.S., Telegin, A.N., Tikhonova, I.M., Verba, M.L., Matveev, Yu.I., Vinnick, A.A., Kopylova, A.V., Dvornikov, L. G., 2000. The results of deep seismic investigations on geotraverses in the Barents Sea from Kola peninsula to Franz-Joseph Land. Tectonophysics, vol. 329, pp. 319–331.

Sakulina, T.S., Roslov, Yu.V., Ivanova, N.M., 2003. Deep Seismic Investigations in the Barents and Kara Seas. Izvestiya, Physics of the Solid Earth, vol. 39, No. 6, pp. 438–452 (Translated from Fizika Zemli, No. 6, 2003, pp. 5–20).

Shipilov, Ed.V., Senin, B.V., 1988. Deep composition of the Barents Sea Shelf bottom Geotectonica, vol. 6, pp. 96–100 (in Russian).

Verba, M.L., 1985. Barents–North Kara Megabasin and its role in evolution of the West-Arctic Shelf. Geological Structure of

the Barents–Kara shelf. PGO Sevmorgeologia, Leningrad, pp. 11–28.

Verba, M.L., Sakoulina, T.S., Telegin, A.N., Atakov, A.I., Matveev, Yu.I, Dvornikov, L.G., Katsev, V.A., Rzhevskiy, N.N., Tikhonova, I.M., 1998. Crust structure in the linking area of the Baltic shield and Barentsevomorskaya shelf plate as presented by complex geophysical investigations on the south segment of the regional geotraverse AR-1. Seismo Geological Model of the Northern Europe Lithosphere. Kola branch of Academy of Sciences USSR, Apatity, pp. 40–81 (in Russian).

Verba, M.L., Ivanova, N.M., Katsev, V.A., Roslov, Yu.V., Sakoulina, T.S., Telegin, A.N., 1999. The results of seismic investigations on regional profiles AR-1 and AR-2 in the Barents and Kara seas. Exploration and Protection of Resources. Nedra, Moscow, pp. 3–7 (in Russian).